Loss of Cellular Inhibitor of Apoptosis Protein 2 Reduces Atherosclerosis in Atherogenic apoE$^{-/-}$ C57BL/6 Mice on High-Fat Diet

Lyne Sleiman, BSc, MSc; Rob Beanlands, PhD, MD;* Mirela Hasu, BSc; Mohamed Thabet, MSc; Alex Norgaard, BSc; YX Chen, MD, PhD; Martin Holcik, PhD;* Stewart Whitman, PhD†

Background—Cellular inhibitor of apoptosis protein 2 (cIAP2) is predicted to participate in atherosclerosis; however, its direct role in atherosclerosis development has not been investigated. We aimed to examine and assess the loss of cIAP2 on atherosclerosis lesion development.

Methods and Results—We used *apoE*$^{-/-}$ C57BL/6 male mice, either cIAP2$^{-/-}$ or cIAP2$^{+/+}$. At 8 weeks, mice were fed a high-fat diet (HFD) for 4 and 12 weeks. Aortic root was serially sectioned and stained with Sudan IV, CD68, α-actin, and terminal deoxynucleotidyl transferase dUTP nick end labeling (TUNEL). *cIAP2*$^{-/-}$ mice displayed a significant decrease in atherosclerotic lesion's macrophage number after 4 weeks of HFD. Similarly, decrease in lesion area at 4 and 12 weeks HFD was detected by use of en face analysis (*cIAP2*$^{-/-}$ 0.58±0.37% versus *cIAP2*$^{+/+}$ 1.51±0.79% [*P*=0.0056]); (*cIAP2*$^{-/-}$ 9.34±4.88% versus *cIAP2*$^{+/+}$ 17.65±6.24% [*P*=0.0019]). Aortic root lesion area after 4 and 12 weeks of HFD also decreased (*cIAP2*$^{-/-}$ 0.0328±0.014 mm^2 versus *cIAP2*$^{+/+}$ 0.0515±0.021 mm^2 [*P*=0.022]); (*cIAP2*$^{-/-}$ 0.3614±0.1157 mm^2 versus *cIAP2*$^{+/+}$ 0.4901±0.125 mm^2 [*P*=0.065]). TUNEL analysis after 4 and 12 weeks of HFD showed a 2.5-fold increase in TUNEL+ cells (*cIAP2*$^{-/-}$ 4.47±2.26% versus *cIAP2*$^{+/+}$ 1.74±0.98% [*P*=0.036]); (*cIAP2*$^{-/-}$ 2.39±0.75% versus *cIAP2*$^{+/+}$ 1.29±0.47% [*P*=0.032]). Smooth muscle cell content in *cIAP2*$^{-/-}$ mice was 3.075±3.3% compared with *cIAP2*$^{+/+}$ with 0.085±0.1% (*P*=0.0071).

Conclusions—Results uncover a key role for cIAP2 in atherosclerotic lesion development, and targeting it may represent a novel therapeutic strategy. (*J Am Heart Assoc.* 2013;2:e000259 doi: 10.1161/JAHA.113.000259)

Key Words: apoptosis • atherosclerosis • C57BL/6 mice • cIAP2

A therosclerosis is a complex inflammatory disease characterized by the accumulation of lipid rich plaques in arterial walls. This response is mediated largely by the recruitment of macrophages to the site of injury.[1] Macro-phages are a major cell type of early atherosclerotic lesions and play important roles during lesion progression stages.[2] One of the vital functions of macrophages is the mediation of apoptotic cell clearance and associated cellular debris through phagocytosis. However, as macrophages become lipid laden, they lose their effective functional ability and undergo apoptosis.[3]

Both antiapoptotic and proapoptotic mechanisms contribute to the development and progression of atherosclerosis, yet the molecular mechanisms leading to the process remain unclear. Because living foam cells play an overall proatherogenic role, the net effect of early lesional macrophage apoptosis is modulation of lesion cellularity and decreased lesion progression.[4] Evidence from disease mouse models lacking antiapoptotic genes such as *Bcl-2* and *AIM* or proapoptotic genes such as *Bax, p19*^{ARF}*,* and *p53* identified a link between apoptosis and disease progression.[5–10]

The inhibitor of apoptosis protein 2 (cIAP2 [also known as HIAP1 or BIRC3]) is a member of the IAP gene family involved

in programmed cell death regulation.[11] IAPs, first identified in baculoviruses, play a key role in the apoptotic signaling pathways.[12,13] IAP proteins share at least 1 cystein-rich domain known as the baculoviral IAP repeat (BIR).[11–13] Eight mammalian IAPs have been discovered to date: BIRC1/NAIP, BIRC2/IAP1/HIAP2, BIRC3/IAP2/HIAP1, BIRC5/survivin, BIRC4/XIAP/hILP, BIRC6/Apollon, BIRC7/ML-IAP, and BIRC8/ILP2.[14] The structure and mechanism of action of cellular IAP2 (cIAP2) have been extensively studied in cancer biology, however, Conte et al[15] showed that macrophages lacking cIAP2 are highly sensitive to apoptosis when stimulated by the inflammatory factor lipopolysaccharide. In addition, it was recently shown that cIAP1 and cIAP2 are critical effectors of the inflamasome.[16] Furthermore, excised human plaques revealed an increase in cIAP2 protein expression levels compared with healthy aorta.[17] Moran and colleagues showed a higher expression of cIAP2 (and caspase-3) in arteries and carotid endarterectomy specimens of symptomatic patients with carotid stenosis compared with the normal carotid arteries of asymptomatic patients.[18] The exact role of cIAP2 in atherosclerosis has remained, however, unclear.

Here, we investigate the consequence of cIAP2 ablation on atheroma development in the widely used apolipoprotein E–null ($apoE^{-/-}$) mouse model of early and late atherosclerosis. We hypothesized that cIAP2 plays a critical role in the early development of atherosclerosis in $apoE^{-/-}$ mice.

Methods

Animals

$cIAP2^{-/-}$ mice (described previously[11]) were bred with atherosclerosis-susceptible $apoE^{-/-}$ mice (Jackson Laboratories). The F3 progeny from the $cIAP2^{-/-} \times apoe^{-/-}$ cross were genotyped, and $cIAP2^{+/+} \times apoe^{-/-}$ and $cIAP2^{-/-} \times apoe^{-/-}$ male littermates were used for experiments. Mice were maintained in the Animal Care Facility at the University of Ottawa Heart Institute. The mice showed no overt phenotypes and appeared healthy up to 52 weeks of age. Mice were divided into 4 groups at 8 weeks of age, where all $cIAP2^{+/+}$ ($cIAP2^{+/+} \times apoE^{-/-}$) and $cIAP2^{-/-}$ ($cIAP2^{-/-} \times apoE^{-/-}$) mice were fed a high-fat diet (HFD) for a period of 4 weeks (early atherosclerosis) or 12 weeks (late atherosclerosis). The diet is a commercially prepared mouse food supplemented with 21% (wt/wt) butterfat, 0.15% (wt/wt) cholesterol, and 19.5% (wt/wt) casein (Dytes Inc). At the end of the dietary period, mice were killed with an overdose of Somnotol, and polymerase chain reaction (PCR) was carried out to confirm genotypes. All animal studies were performed in accordance with the policies and guidelines of the University of Ottawa Animal Care Committee.

Bone Marrow–Derived Macrophage Collection and Cell Culture

Bone marrow–derived macrophages (BMDMs) were collected from $cIAP2^{-/-}$ (n=3) and $cIAP2^{+/+}$ (n=3) mice as previously described.[19,20] DMEM containing 10% FBS, 1% penicillin/ streptomycin, and 10 ng/mL macrophage-colony stimulating factor (Peprotech) was used to seed 4×10^5 cells/well onto a 96-well plate. Following the culture period, tumor necrosis factor (TNF)α (Invitrogen) was added to the plates at concentrations of 0.02, 10, 50, and 100 ng/mL for 48 hours.

Cell Viability Assay

Cell viability was assessed using the 3-(4,5-dimethyl-thiazol-2-yl)-2,5-diphenyltetrazolium bromide (MTT) assay (Sigma) as previously described.[21] Absorbance was read at 570 nm using SynergyMx microplate spectrometer (BioTek) and Gen5 2.0 software (BioTek Institute).

Tissue Collection

Following the dietary period, all mice were killed and perfused with cold $1\times$ PBS via puncture to the left ventricle with the perfusate being drained from the severed right atrium. The hearts were separated from the aorta at the base, embedded in optimum cutting temperature compound, and stored at $-20°C$.

Quantification of Atherosclerotic Lesions

To assess the differences in atherosclerotic lesions size between the $cIAP2^{-/-}$ and $cIAP2^{+/+}$ groups, en face lesion analysis was carried out after both 4 and 12 weeks of HFD.

Aortas from killed mice were exposed as described previously.[22] The aorta was pinned onto dissecting wax, stained with Sudan IV, and photographed at a fixed magnification. The total aortic areas and lesion areas were subsequently calculated using ImagePro 6.1 Software (Media Cybernetic). Final results are reported as a percentage of the total area of the aortic arch and descending aorta–containing lesions.

To determine atherosclerotic size within the ascending aorta, the mean lesion area was derived from 4 serial Sudan IV–stained sections, cut 10 μm thick and collected 100 μm apart over a 1-mm segment of the aortic root. The mean lesion area was taken as the lesion size for each mouse, and analysis of the lesions was carried as described previously.[22] Images were created using the digital CoolSNAP cf camera (Roper Scientific Inc) using ImagePro software (Media Cybernetic).

Blood Sampling and Plasma Cholesterol Analysis

Terminal blood samples were collected in EDTA-coated tubes by puncture to the right ventricle. Plasma was collected from

all mouse groups (n=14/group), and subsequently total cholesterol levels were determined with the use of enzymatic assay kits. A colorimetric assay (Cholesterol E; Wako Bioproducts) was used to determine serum total cholesterol concentrations present in terminal blood samples. Lipoprotein cholesterol distributions were evaluated in individual serum samples (60 μL) via fast protein liquid chromatography (FPLC) separation. Serum samples from 5 mice per group were evaluated, and the mean values for each group were plotted and compared.

Terminal Deoxynucleotidyl Transferase dUTP Nick End Labeling Staining

A red in situ apoptosis detection kit, ApopTag, was used to label DNA-synthesizing cells according to manufacturer's protocol (Chemicon). Images (n=7 mice/group) were captured by the use of SpotBasic software (Diagnostic Instruments, Inc). Four serial sections were quantified in the aortic valve region at 100-μm intervals. Only terminal deoxynucleotidyl transferase dUTP nick end labeling (TUNEL)-positive nuclei were included that displayed nuclear fragmentation and DAPI staining. The number of DAPI- and TUNEL-positive nuclei was counted using the ImageJ 1.45s software under a fluorescent microscope ($\times$20). Numbers of TUNEL-positive nuclei are expressed as a percentage of the total cell number in the lesion for each individual mouse.

Immunohistochemistry

The extent of macrophage infiltration in atherosclerotic lesions was determined through CD68-positive staining analysis. Samples were incubated with anti-CD68 primary antibody (1:100; Serotec). To quantify CD68 content within the ascending aorta, the mean lesion area was derived from 4 serial CD68-stained sections. The sections are 10 μm from the previously used Sudan IV–stained sections. This enables the analysis and quantification of CD68 to be easily compared through analysis of previous sections stained with Sudan IV. The mean lesion area was taken as the lesion size for each mouse. To determine the extent of smooth muscle cells (SMCs) in the aortic root atherosclerotic lesions, frozen sections were incubated with anti–smooth muscle actin (1:20; Sigma) using SIGMA*FAST* substrate (Sigma). α-Actin–positive regions within the atherosclerotic lesions were represented as a percentage of total lesion area.

Statistical Analysis

Statistical calculations were carried out using SAS software (version 9.2, SAS Institute Inc). Continuous measures are presented as means±SD. Nonparametric Wilcoxon rank sum tests were used for comparisons. A value of $P<0.05$ was considered statistically significant. Power calculations from previous similar studies indicate that the outlined experiments would use a sufficient number of animals (n=15) to attain a power of 0.8 for 20% change in lesion and provide statistically reliable results if no effects of atherosclerosis are observed. All data were analyzed by a second observer who was blinded to the study.

Results

In Vitro Cell Viability Assay

BMDMs from $cIAP2^{-/-}$ mice are more sensitive to TNFα-induced apoptosis than are $cIAP2^{+/+}$ BMDMs in vitro. Figure 1A shows the relative viability of BMDMs from 4-week HFD mice exposed to varying TNFα concentrations (0, 0.2, 10, 50, and 100 ng/mL). As indicated in the figure, $cIAP2^{-/-}$ BMDMs are more sensitive to TNFα-induced apoptosis than are $cIAP2^{+/+}$ BMDMs, with significant differences observed at 50 and 100 ng/mL ($P<0.001$). A similar trend is observed in BMDMs from mice on a 12-week HFD, as seen in Figure 1B. $cIAP2^{-/-}$ BMDMs have lower viability when exposed to increasing TNFα concentrations compared with $cIAP2^{+/+}$ BMDMs, with significant differences observed at 50 ng/mL ($P=0.027$) and at 100 ng/mL ($P<0.001$).

Early and Late Atherosclerotic Lesions in Ascending and Descending Aorta

$cIAP2$ gene deletion resulted in reduced early atherosclerosis burden in the experimental group compared with $cIAP2^{+/+}$ on a 4-week HFD. As shown in Figure 2A, the $cIAP2^{-/-}$ group (n=10, 0.58±0.37%) showed a significant decrease in lesion area compared with the $cIAP2^{+/+}$ group (n=13, 1.51±0.79%). This decrease in lesion size translates into a 60.7% difference ($P=0.0056$). Representative images are shown in Figure 2B. Deletion of the $cIAP2$ gene resulted in reduced late atherosclerosis burden in the experimental group compared with $cIAP2^{+/+}$ on a 12-week HFD. As shown in Figure 3A, the $cIAP2^{-/-}$ group showed a significant reduction in lesion area (n=17, 9.34±4.88%) versus the control $cIAP2^{+/+}$ group (n=15, 17.65±6.24%). This reduction in lesion size translates into a 53% difference ($P=0.0019$). Figure 3B shows representative images.

Early and Late Atherosclerotic Lesions in Aortic Root

$cIAP2$ gene deletion resulted in reduced early atherosclerosis burden in the experimental group compared with the wild-type $cIAP2^{+/+}$ controls on a 4-week HFD. As shown in Figure 2C, $cIAP2^{-/-}$ mice showed a significant reduction in the average
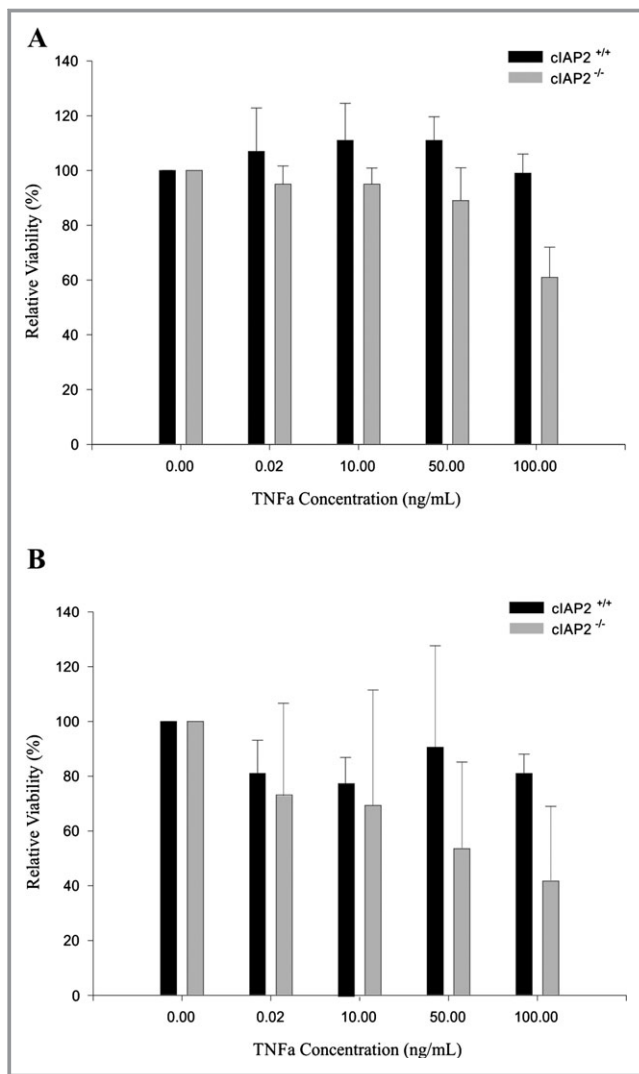
Figure 1. *cIAP2* deletion increases bone-marrow derived macrophage sensitivity to TNFα-induced apoptosis. A, Relative viability (%) of *cIAP2*$^{+/+}$ BMDMs from mice on a 4-week HFD compared with BMDMs from *cIAP2*$^{-/-}$ with significant difference observed at 50 and 100 ng/mL, *P*<0.001. B, Relative viability of *cIAP2*$^{+/+}$ BMDMs of mice on a 12-week HFD compared with BMDM from *cIAP2*$^{-/-}$ mice with significant differences observed at 50 ng/mL (*P*=0.027) and at 100 ng/mL (*P*<0.001). BMDM indicates bone marrow–derived macrophage; HFD, high-fat diet; TNF, tumor necrosis factor.

lesion area (n=11, 0.0328±0.014 mm^2) versus *cIAP2*$^{+/+}$ mice (n=14, 0.0515±0.021 mm^2), (*P*=0.022). Representative images from the aortic root analysis are shown in Figure 2D. *cIAP2* gene deletion resulted in reduced late atherosclerosis burden in the experimental group compared with *cIAP2*$^{+/+}$ on a 12-week HFD. As shown in Figure 3C, *cIAP2*$^{-/-}$ mice showed a reduction (trending towards significance) in average lesion area (n=11, 0.3614±0.157 mm^2) versus the control *cIAP2*$^{+/+}$ mice (n=12, 0.4901±0.125 mm^2), (*P*=0.065). Figure 3D shows representative images.

Plasma Lipoprotein and Cholesterol Levels

There were no significant differences in the serum total cholesterol levels at the end of the study (Figure 4).

Apoptosis Quantification by TUNEL Staining

To examine the role *cIAP2* deletion plays in the atherosclerotic lesions apoptosis, TUNEL analysis was performed. Aortic root sections were stained with TUNEL and DAPI. Cells showing nuclear condensation with DAPI and TUNEL were counted as TUNEL+ cells in the analysis. TUNEL+ cells showing no nuclear condensation using DAPI were mostly concentrated in the necrotic cores and not considered in the analysis. The atherosclerotic lesions of *cIAP2*$^{-/-}$ mice on a 4-week HFD showed an increased number of apoptotic cells compared with wild-type mice. Figure 5A shows the *cIAP2*$^{-/-}$ (n=6) mice with 4.47±2.26% apoptosis in their early atherosclerotic lesions compared with the wild-type *cIAP2*$^{+/+}$ (n=7) with 1.74±0.98% (*P*=0.036). Aortic root lesions analysis of mice on a 12-week HFD show a higher apoptosis percentage in the *cIAP2*$^{-/-}$ mice. Figure 5C shows *cIAP2*$^{-/-}$ (n=8) mice with 2.39±0.75% apoptosis compared with wild-type *cIAP2*$^{+/+}$ (n=5) mice with 1.29±0.47% (*P*=0.032). Representative images of the DAPI and TUNEL analysis are shown in Figure 5B and 5D.

Macrophage and SMC Content

To examine the effect of *cIAP2* deletion on atherosclerotic lesion's macrophage content, aortic root sections were stained with CD68—a marker of active macrophages. As shown in Figure 6A, *cIAP2*$^{-/-}$ mice showed a trend for reduction in average lesion area compared with the *cIAP2*$^{+/+}$ (*cIAP2*$^{-/-}$ mice, n=6 [0.0306±0.0080 mm^2] versus *cIAP2*$^{+/+}$ mice, n=5 [0.0485±0.0210 mm^2] [*P*=0.068]). Lesion analysis for CD68 and Sudan IV staining from 4-week *cIAP2*$^{-/-}$ and *cIAP2*$^{+/+}$ groups were overlapped to examine the relation between lesion macrophage infiltration and lipid staining. A trend is seen in CD68 macrophage and Sudan IV staining for the 4-week *cIAP2*$^{+/+}$ group. The *cIAP2*$^{-/-}$ mice had a CD68 macrophage average staining area of 0.0356±0.0142 mm^2 and Sudan IV–stained average area of 0.0327±0.0141 mm^2. *cIAP2*$^{+/+}$ mice had a CD68 macrophage average staining area of 0.0485±0.0216 mm^2 and Sudan IV–stained average area of 0.0501±0.0246 mm^2. Figure 6B shows representative images from this analysis. Figure 6C shows the correlation between CD68 and Sudan IV staining for 4-week *cIAP2*$^{-/-}$ and *cIAP2*$^{+/+}$ mice. There is a strong correlation between the 2 parameters (Pearson correlation, R^2=0.99).

The effect of cIAP2 deletion on SMC content in the plaque was examined by performing immunohistochemical analysis
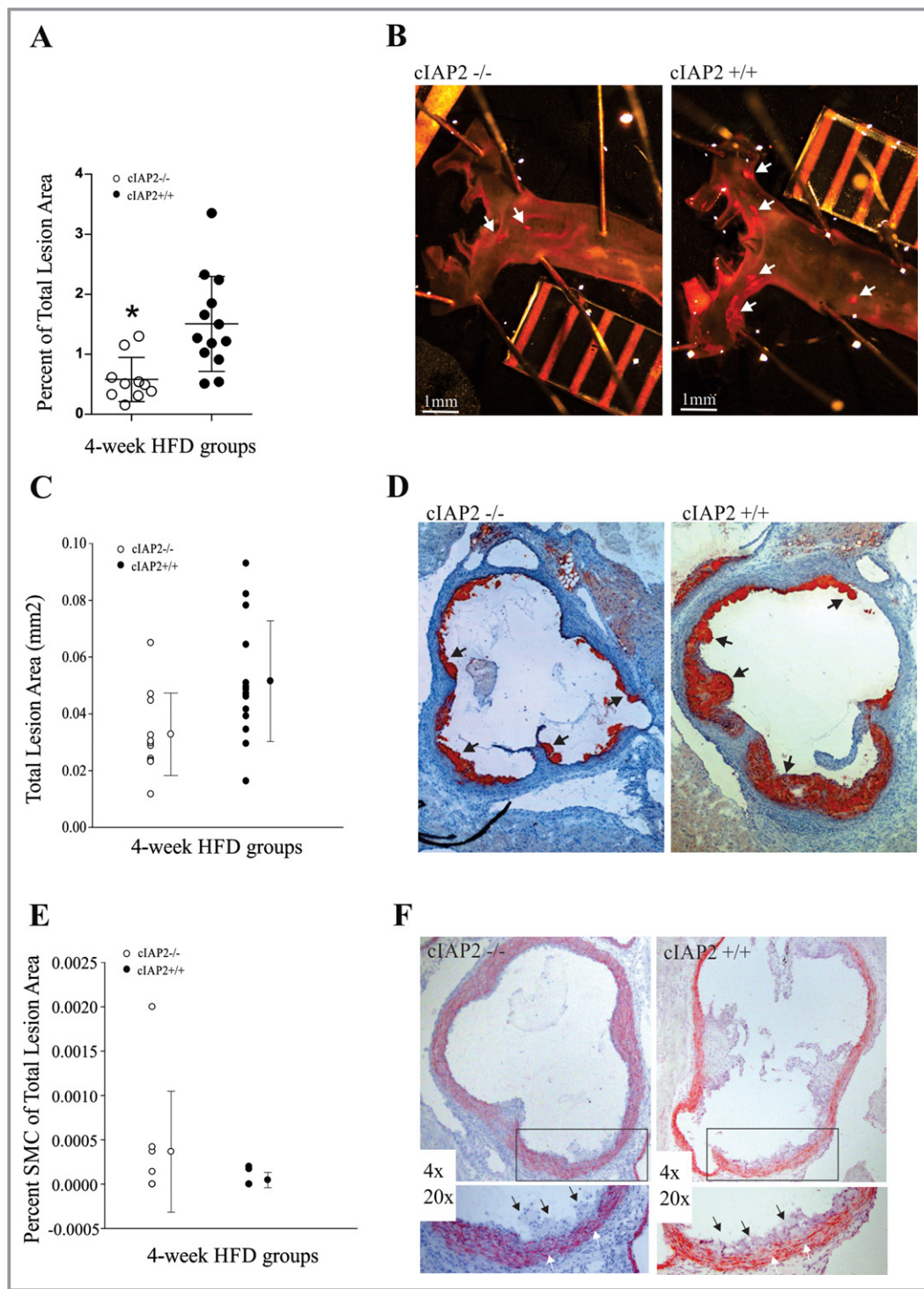
Figure 2. *cIAP2* deletion reduces early atherosclerosis in *apoE*$^{-/-}$ on a 4-week HFD. A, Scatterplot of lesion area represented as a percentage of total aorta area. *cIAP2*$^{-/-}$ mice show a significant reduction in lesion area of 0.58±0.37% (n=10) vs 1.51±0.79% (n=13) for *cIAP2*$^{+/+}$ mice (*P=0.0056). B, Representative images of en face aorta from *cIAP2*$^{-/-}$ (left) and *cIAP2*$^{+/+}$ (right) mice. En face aortas are stained with Oil-Red-O, and the lesion area is indicated with a white arrow. C, Scatterplot showing means of lesion size (mm^2) ±SD along with the average of the means. *cIAP2*$^{-/-}$ mice show a significant reduction in lesion area of 0.0328±0.014 mm^2 (n=11) vs *cIAP2*$^{+/+}$ mice of 0.0515±0.021 mm^2 (n=14) (*P=0.022). D, Representative aortic root histological image of a *cIAP2*$^{-/-}$ (left) and *cIAP2*$^{+/+}$ (right) mice (original magnification ×10). Sudan IV–stained aortic root sections; white arrows indicate lesions. E, Scatterplot of SMC content as a percentage of total lesion area along with the average of the means. SMC content is negligible for both groups. F, Representative images of α-SMC staining visible in red for 4-week HFD *cIAP2*$^{-/-}$ (left panel) and *cIAP2*$^{+/+}$ (right panel). White arrows indicate SMC in the lumen, and black arrows point toward the lesion area. HFD, high-fat diet; SMC, smooth muscle cell.
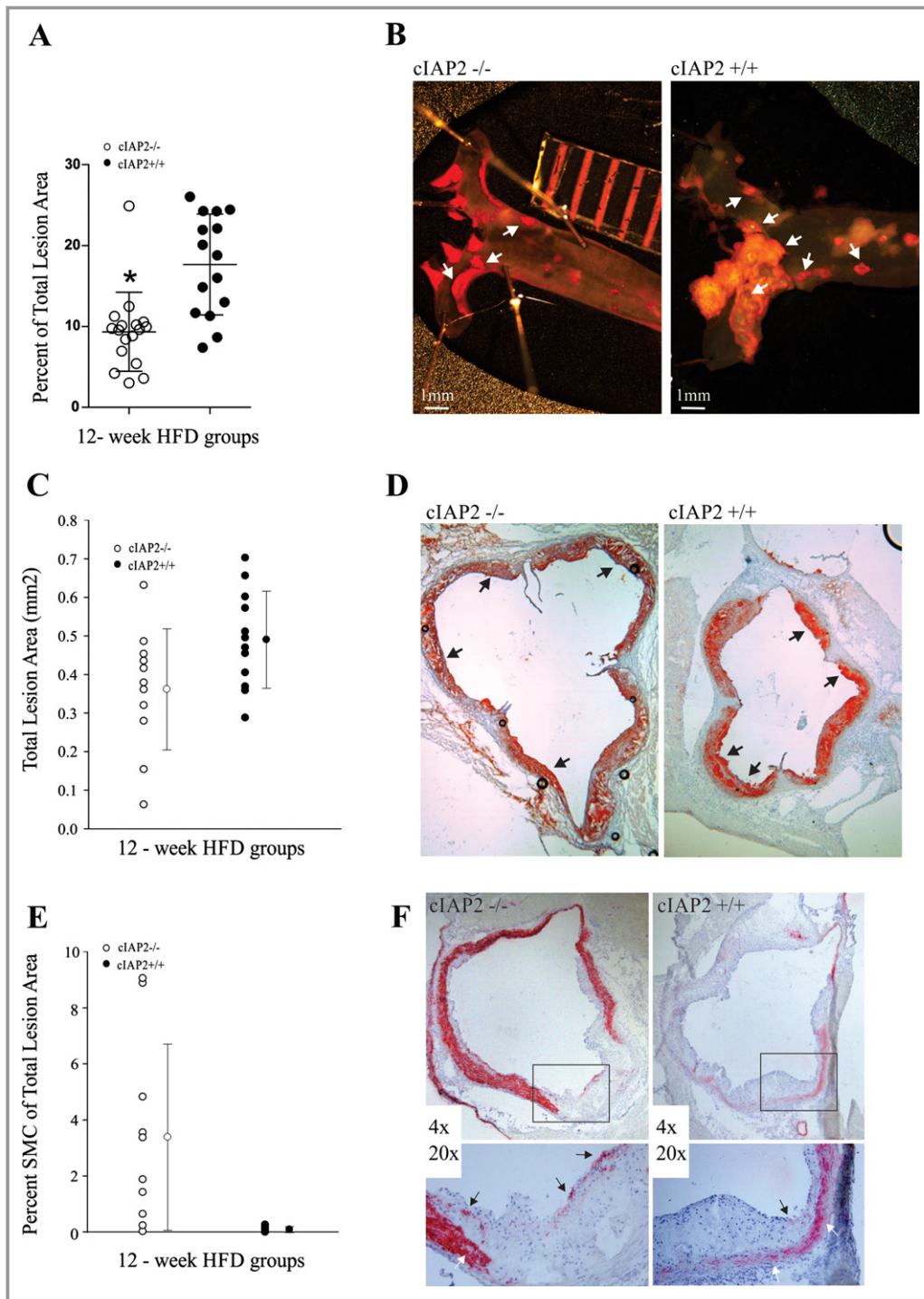
Figure 3. *cIAP2* deletion reduces early atherosclerosis in *apoE*$^{-/-}$ on a 12-week HFD. A, Scatterplot of lesion area represented as a percentage of total aorta area. *cIAP2*$^{-/-}$ mice show a significant reduction in lesion area of 9.34±4.88% (n=17) vs 17.65±6.24% (n=15) for *cIAP2*$^{+/+}$ mice (*P=0.0019). B, Representative image of en face aortas from *cIAP2*$^{-/-}$ (left) and *cIAP2*$^{+/+}$ (right) mice. En face aortas were stained with ORO, and the lesion area is indicated with a white arrow. The scale represents millimeters for reference. C, Scatterplot showing means of lesion size (mm^2) ±SD along with the average of the means. The *cIAP2*$^{-/-}$ mice show a reduction (trending toward significance) in lesion area of 0.3614±0.157 mm^2 (n=11) vs 0.4901±0.125 mm^2 (n=12) for *cIAP2*$^{+/+}$ mice (P=0.065). D, Representative aortic root histological image of a *cIAP2*$^{-/-}$ (left) and *cIAP2*$^{+/+}$ (right) mice (original magnification ×10). Sudan IV–stained aortic root sections; white arrows indicate lesion area. E, Scatterplot of SMC content as a percentage of total lesion area along with the average of the means. Percentage of SMC content for *cIAP2*$^{-/-}$ (n=11) is 3.075±3.3% compared with 0.085±0.1% for *cIAP2*$^{+/+}$ (n=11) (P=0.0071). F, Representative images of α-SMC staining visible in red for 12-week HFD: *cIAP2*$^{-/-}$ (left panel) and *cIAP2*$^{+/+}$ (right panel). White arrows indicate SMC in the lumen, and black arrows point toward the SMC in the lesion area. HFD indicates high-fat diet; SMC, smooth muscle cell.
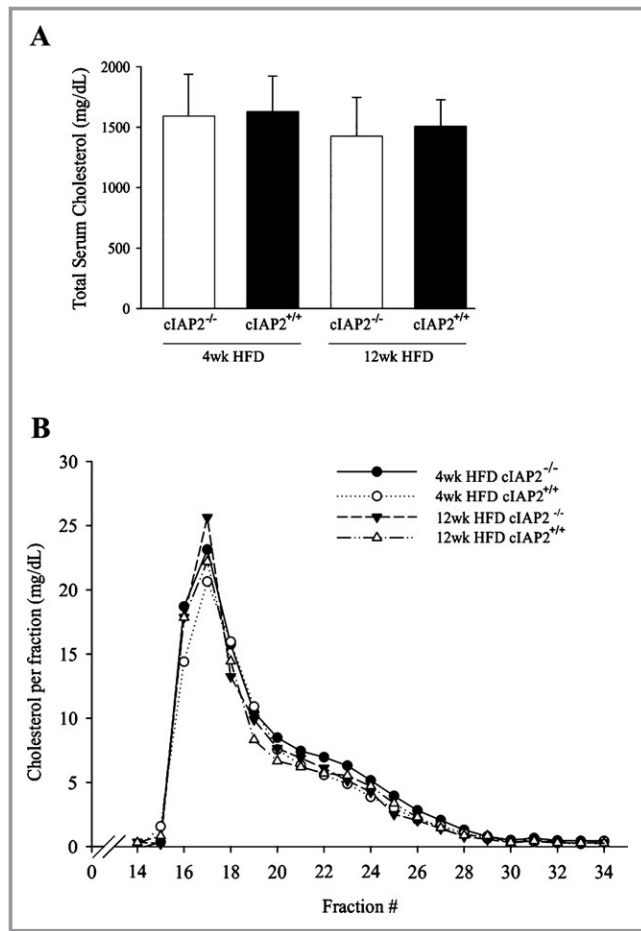
Figure 4. Plasma lipoprotein and cholesterol levels are not affected in $cIAP2^{-/-}$ animals. A, Total serum cholesterol levels as determined at the end of the study in each treatment group. B, Lipoprotein cholesterol profiles were determined at the end of the study in each treatment group by use of size exclusion chromatography (FPLC). FPLC indicates fast protein liquid chromatography; HFD, high-fat diet.

on aortic root sections using anti–α-actin antibody. As shown in Figure 2E, the content of SMCs in the lesions was negligible in both the $cIAP2^{-/-}$ and $cIAP2^{+/+}$ mice on a 4-week HFD (P=0.22). Figure 3E shows the average percentage of SMCs in $cIAP2^{-/-}$ (n=11) was 3.075±3.3% compared with 0.085±0.1% for $cIAP2^{+/+}$ (n=11) (P=0.0071). Figures 2F and 3F show SMC content in aortic root of mice on a 4- and 12-week HFD.

Discussion

In the present study, we investigated a role for cIAP2 in early and late atherosclerotic lesion development in an $apoE^{-/-}$ mouse model. Detailed analysis of atherosclerosis in the aortic root and the ascending and descending aorta revealed a significant reduction in the atherosclerosis burden of $cIAP2$-deleted mice at both time points. The reduction in

atherosclerosis coincides with an increase in macrophage apoptosis in the $cIAP2$-deleted mice in both the early and late stages of the disease. The changes in lesional cell death were accompanied by a trend for a decrease in macrophage content at the early stages of the disease. Loss of cIAP2 promoted SMC content in aortic root lesions. $cIAP2$ deletion did not affect serum cholesterol and lipoprotein contents compared with wild-type mice. This study demonstrates the role cIAP2 plays as a major mediator of lesion cellularity and macrophage apoptosis. Inhibition of this pathway results in a shift toward more cellular apoptosis, affecting lesion composition and leading to reduced plaque size at the time points studied.

Evidence for a Role for cIAP2 in Apoptosis and Atherosclerosis

The role of cIAP2 has not been carefully examined in atherosclerosis. Early evidence exists suggesting a role in atherosclerosis. A study in the late 1990s by J.G. Horrevoets and colleagues[23] revealed an overexpression of cIAP2 in the endothelial lining of atherosclerotic aorta coinciding with MCP-1 expression. Further evidence by Moran and Agrawal[18] shows elevated expression of cIAP2 in human excised symptomatic plaques that paralleled caspase-3 expression, suggesting a role in apoptosis. Early work by Ciu et al and later work by Conte et al demonstrate that lipopolysaccharide treatment upregulates cIAP2 in macrophages and that lipopolysaccharide-stimulated $cIAP2^{-/-}$ macrophages are highly susceptible to apoptosis.[15,24] $cIAP2$ deletion elicited potent effects on macrophage viability, suggesting a crucial role of macrophages maintainance during an inflammatory response. Collectively, these studies suggest a central involvement of cIAP2 in atherosclerotic plaques macrophage viability, supporting the data represented in this study. Previous studies have suggested a role for cIAP2 in macrophage viability and atherosclerosis; however, we demonstrate, for the first time, a direct role for cIAP2 in reducing early and late atherosclerotic lesion size in an $apoE^{-/-}$ mouse model.

Elevated TNF levels have been reported in the carotid plaques of symptomatic patients.[25,26] Mahoney et al[27–30] show that cIAP2 might be able to regulate TNFα-mediated nuclear factor–$\kappa\beta$ activation, inducing a variety of proapoptotic and antiapoptotic genes. These authors also report that cells lacking cIAP1/2 were greatly sensitized to apoptosis on exposure to TNFα. Hence, we examined the effect of cIAP2 loss on BMDM sensitivity on exposure to varying exogenous TNFα concentrations. As shown in Figure 1, macrophages lacking cIAP2 are more sensitive to apoptosis, indicated by loss of viability with increasing TNFα concentrations. These results can potentially explain the increase in apoptosis
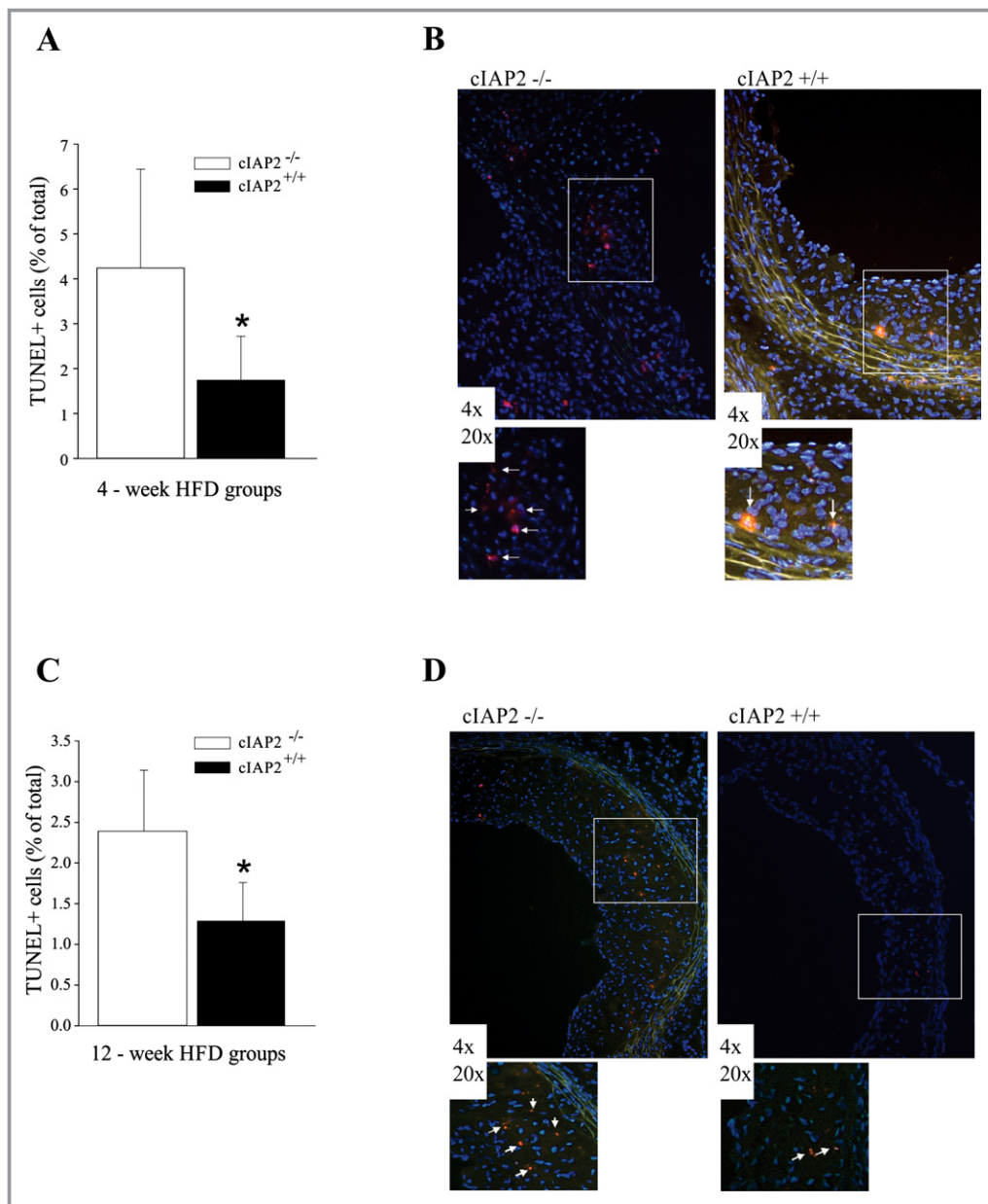
Figure 5. *cIAP2* deletion increases apoptosis in early atherosclerotic lesions of *apoE*$^{-/-}$ after a 4-week HFD. A, Bar graph showing the mean percentage of TUNEL+ cells. *cIAP2*$^{-/-}$ (n=6) mice show a significant increase in TUNEL+ cells with 4.47±2.26% vs *cIAP2*$^{+/+}$ (n=7) mice with 1.74±0.98% (*P*=0.036). B, Aortic root sections from *cIAP2*$^{-/-}$ (left) and *cIAP2*$^{+/+}$ (right) mice. *cIAP2* deletion increases apoptosis in late atherosclerotic lesions of *apoE*$^{-/-}$ after a 12-week HFD. C, Bar graph showing the mean percentage of TUNEL+ cells. The *cIAP2*$^{-/-}$ (n=8) mice show a significant increase in TUNEL+ cells with 2.39±0.75% vs *cIAP2*$^{+/+}$ (n=5) mice with 1.29±0.47% (*P*=0.032). D, Aortic root sections from *cIAP2*$^{-/-}$ (left) and *cIAP2*$^{+/+}$ (right) mice. Apoptotic cells (in red) are indicated with a white arrow. HFD indicates high-fat diet; TUNEL, terminal deoxynucleotidyl transferase dUTP nick end labeling.

detected with TUNEL staining in both early and late atherosclerosis (Figure 5) along with the reduced macrophage content in the plaque (Figure 6). Zheng and colleagues[30] show that cIAP2 is part of the TNF-induced TNFR1 signaling complex, which is vital in the regulation of the nuclear factor–κβ proinflammatory transcription pathway. TNFα was also shown to induce cIAP2 expression sufficiently to inhibit TNFα-induced cell death.[28] Furthermore, a recent study by McComb et al[31] shows that reduced cIAP activity led to increased macrophage cell death in vivo. Collectively, previous findings along with data represented in our study indicate a strong role for cIAP2 in limiting atherosclerotic macrophage cell death, possibly via a TNFα-induced apoptotic pathway.
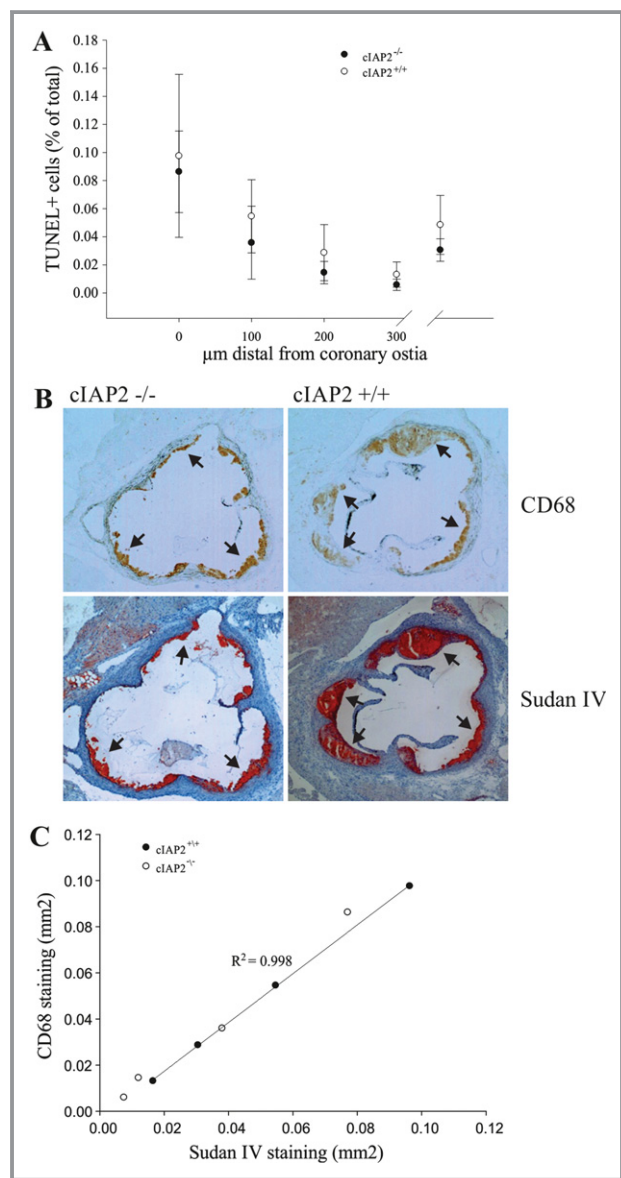
Figure 6. *cIAP2* deletion reduces macrophage content in early atherosclerotic plaque of *apoE*$^{-/-}$ mice on 4-week HFD. A, Scatterplot showing mean of CD68+ lesion size at each of the aortic root levels (mm^2) ±SD along with the average of the means. The *cIAP2*$^{-/-}$ mice show a reduction (trending toward significance) in CD68+ lesion area of 0.0306±0.008 mm^2 (n=6) vs 0.0485±0.021 mm^2 (n=5) for *cIAP2*$^{+/+}$ mice. B, Representative histological image of aortic root of a *cIAP2*$^{-/-}$ mouse (left) and *cIAP2*$^{+/+}$ mouse (right) (original magnification ×10). Aortic root sections were stained with CD68 (top panel) and Sudan IV (bottom panel), and the lesion area is indicated with a black arrow. C, Scatterplot representing the correlation between the CD68 staining measurements and Sudan IV staining measurements for *cIAP2*$^{-/-}$ and *cIAP2*$^{+/+}$ mice after a 4-week Western diet. CD68 lesion areas (mm^2) were plotted on the *y*-axis vs Sudan IV–stained areas (mm^2) plotted on the *x*-axis. The Pearson correlation coeffient for *cIAP2*$^{-/-}$ and *cIAP2*$^{+/+}$ data points is R^2=0.99. The straight line represents the line of best fit. TUNEL indicates terminal deoxynucleotidyl transferase dUTP nick end labeling.

The Role of cIAP2 in Early Atherosclerotic Lesions

Macrophage apoptosis normally takes place in early atherosclerotic lesions, possibly through 1 or more pathways involving proapoptotic proteins *p53* and *Bax*.[32,33] Arai et al[7] examined the role of AIM loss (an inhibitory factor) on early atherosclerotic lesions, showing reduced early atherosclerotic lesions in *AIM*$^{-/-}$ mice compared with the *AIM*$^{+/+}$ in an *LDLr*$^{-/-}$ mouse model. These studies demonstrate the limiting effect of apoptosis on lesion cellularity and progression in early lesion foam cells. In parallel, the present study shows reduced early-stage lesion content in *cIAP2*$^{-/-}$ × *apoE*$^{-/-}$ compared with wild-type mice, as shown in Figure 1. To determine whether apoptosis plays a role in lesion size reduction, we used TUNEL analysis to detect the percentage of apoptotic cells within early lesions. The reduction in atherosclerotic lesion size was accompanied by an increase in apoptosis represented by an increase in the percentage of TUNEL+ cells within the lesions (Figure 5). Increased cellular apoptosis in early atherosclerotic lesions may have an effect on the number of macrophages predominantly present in early plaque. Therefore, we further examined the role of *cIAP2* deletion on macrophage content in early atherosclerotic plaque by combining macrophage CD68 immunohistochemistry analysis and Sudan IV–stained aortic root sections. These data showed a reduction in CD68+ macrophages that correlated with reduced lesion size (Figure 6).

The effect of cIAP2 loss on early plaque SMC content was examined using α-actin immunohistochemistry analysis on aortic root sections of mice on a 4-week HFD. SMCs were virtually absent in both study groups where atherosclerotic lesions are at early stage III of the disease, mainly composed of macrophages.[34] We propose, based on both our current data and previous evidence, that *cIAP2* deletion resulted in increased macrophage apoptosis in the atherosclerotic lesions leading to reduced CD68$^+$ cells or macrophages in early lesions and resulting in reduced plaque size as seen in the aortic root and ascending and descending aortas. Increased lesional apoptosis translates into an efficient clearance process whereby phagocytes rapidly and safely clear apoptotic bodies from early lesions.

The Role of cIAP2 in Advanced Lesions

Despite differences in lesion stages amongst the study groups, a similar trend was observed regarding the reduction in atherosclerotic plaque size. Figure 2 demonstrates that *cIAP2*$^{-/-}$ mice on a 12-week HFD have reduced lesion area compared with the *cIAP2*$^{+/+}$ mice when examining the aortic root and ascending and descending aortas. As the mice are placed on a prolonged HFD, the

atherosclerotic plaque burden increases.[34] However, the *cIAP2*^{−/−} mice still maintain a reduced lesion size compared with the *cIAP2*^{+/+} group. This confirms the notion that finding the right target for reducing atherosclerosis progression at an early stage could help reduce the progression of advanced lesions. Such an early intervention may be expected to reduce the chance of plaque rupture and thrombus formation that lead to strokes and myocardial infarctions.

A large number of apoptotic cells were found in excised human aorta as a result of poor phagocytic clearance.[35] Similarly, we found a higher percentage of apoptotic cells in the advanced plaque of *cIAP2*^{−/−} mice, indicative of poor phagocytic clearance (Figure 5). SMC accumulation is implicated in plaque development, as opposed to SMC apoptosis, which is linked to plaque rupture, coagulation, and calcification.[36,37] Work by Moran and Agrawal[18] noted increased SMC-actin expression in carotid endarterectomy of asymptomatic patients, whereas cIAP2 was overexpressed in specimens of symptomatic patients. Interestingly, the *cIAP2*^{−/−} mice show significantly higher SMC content, resembling fibrous cap formation in the atherosclerotic lesions, compared with the *cIAP2*^{+/+} mice (Figure 3F). These findings point toward a novel atheroprotective role for cIAP2 loss that has not been previously documented. Chronic vascular SMC apoptosis in *apoE*^{−/−} mice resulted in reduced plaque vascular SMC content and promoted plaque calcification, medial degeneration, and stenosis.[37] Furthermore, *apoE*^{−/−} mice receiving progenitor SMCs had reduced macrophage content along with increased plaque collagen and SMCs collectively restricting plaque development and promoting plaque stability.[38] Interestingly, the absence of macrophage tumor suppressor gene *p53* in advanced lesions did not affect SMC content.[10] Despite the reduction in atherosclerosis following AIM deletion, there was no documented effect on SMC content in the plaque.[8] cIAP2 loss reduced macrophage content in the plaque, resulting in reduced protease and cytokine production from macrophages.[39] This could potentially explain the higher SMC content in the *cIAP2*^{−/−} plaque protecting against destabilizing effects. These results highlight the unique effect of cIAP2 on SMC plaque content and its potential ability to promote stable plaque formation.

Despite lack of previous evidence linking cIAP2 to plaque SMC content, sufficient evidence points to the stabilizing effect of atherosclerotic plaque SMCs.[18,38,40,41] Data from the present study suggest that cIAP2 loss increases fibrous plaque SMC content, providing an atheroprotective mechanism for plaque stabilization and prevention of further rupture. More work needs to be done to examine the extent to which cIAP2 loss contributes to multiple factors involved in fibrous cap formation.

Possible Therapeutic Implications

The results presented here suggest that antagonizing the expression and/or function of cIAP2 may have therapeutic benefits in patients during the early stages of atherosclerosis. The suppression and/or inhibition of IAPs can oversensitize cancerous cells to diverse proapoptotic therapeutics. Inhibition of the caspase-dependent pathway requires antagonism of the IAP-mediated pathway achieved by the cytosolic releases of endogenous Smac/DIABLO in response to proapoptotic stimuli.[42–44] Molecular mechanistic studies examining smac-mimetics sensitive to cIAP2 hold promise for novel therapeutic drug-enhancing cancer treatment responses.[45,46] Smac-mimetic drugs have been patented and used against X-linked inhibitor of apoptosis (XIAP), cellular inhibitor of apoptosis protein (cIAP1), cIAP2, and Survivin.[47,48]

We propose that, in addition to the potential cancer applications, cIAP2-specific Smac-mimetic drugs hold a promising future in reducing early atherosclerotic lesion development and serve an atheroprotective role. cIAP2 inhibition will act, as in the *cIAP2* knock-out mouse model, to induce early lesion macrophage apoptosis reducing atherosclerotic lesion cell number and size and promoting more stable plaque formation. Being able to reduce plaque size and progression could translate into effective therapy to prevent detrimental clinical implications of plaque rupture such as strokes and myocardial infarction.

Disclosures

None.

References

1. Glass CK, and Witztum JL. Atherosclerosis: the road ahead. *Cell*. 2001;104:503–516.
2. Ley K, Miller YI, Hedrick CC. Monocyte and macrophage dynamics during atherogenesis. *Arterioscler Thromb Vasc Biol*. 2011;31:1506–1516.

3. Kockx MM. Apoptosis in the atherosclerotic plaque: quantitative and qualitative aspects. *Arterioscler Thromb Vasc Biol*. 1998;18:1519–1522.

4. Tabas I. Consequences and therapeutic implications of macrophage apoptosis in atherosclerosis: the importance of lesion stage and phagocytic efficiency. *Arterioscler Thromb Vasc Biol*. 2005;25:2255–2264.

5. Kutuk O, Basaga H. Bcl-2 protein family: implications in vascular apoptosis and atherosclerosis. *Apoptosis*. 2006;11:1661–1675.

6. Meilhac O, Escargueil-Bland I, Thiers J-C, Salvayre R, Negre-Salvayre A. Bcl-2 alters the balance between apoptosis and necrosis, but does not prevent cell death induced by oxidized low density lipoproteins. *FASEB J*. 1999;13:485–494.

7. Arai S, Shelton JM, Chen M, Bradley MN, Castrillo A, Bookout AL, Mak PA, Edwards PA, Mangelsdorf DJ, Tontonoz P, Miyazaki T. A role for the apoptosis inhibitory factor AIM/Spα/Api6 in atherosclerosis development. *Cell Metab*. 2005;1:201–213.

8. Liu J, Thewke DP, Su YR, Linton MF, Fazio S, Sinensky MS. Reduced macrophage apoptosis is associated with accelerated atherosclerosis in low-density lipoprotein receptor-null mice. *Arterioscler Thromb Vasc Biol*. 2005;25:174–179.

9. Gonza'lez-Navarro H, Abu Nabah YN, Vinué Á, Andrés-Manzano MJ, Collado M, Serrano M, Andrés V. p19ARF deficiency reduces macrophage vascular smooth muscle cell apoptosis and aggravates atherosclerosis. *J Am Coll Cardiol*. 2010;55:2258–2268.

10. Boestena LSM, Zadelaarb ASM, van Nieuwkoopa A, Hua L, Teunissec AFAS, Jochemsenc AG, Eversf B, van de Waterg B, Gijbels MJJ, Van Vlijmend BJM, Havekes LM, De Wintherh MPJ. Macrophage p53 controls macrophage death in atherosclerotic lesions of apolipoprotein E in deficient mice. *Atherosclerosis*. 2009;207:399–404.

11. Liston P, Roy N, Tamai K, Lefebvre C, Baird S, Cherton-Horvat G, Farahani R, McLean M, Ikeda JE, MacKenzie A, Korneluk RG. Suppression of apoptosis in mammalian cells by NAIP and a related family of IAP genes. *Nature*. 1996;379:349–353.

12. Salvesen GS, Duckett CS. IAP proteins: blocking the road to death's door. *Nat Rev Mol Cell Biol*. 2002;3:401–410.

13. Duckett CS, Nava VE, Gedrich RW, Clem RJ, Van Dongen JL, Gilfillan MC, Shiels H, Hardwick JM, Thompson CB. A conserved family of cellular genes related to the baculovirus iap gene and encoding apoptosis inhibitors. *EMBO J*. 1996;15:2685–2694.

14. Deveraux QL, Reed JC. IAP family proteins—suppressors of apoptosis. *Genes Dev*. 1999;13:239–252.

15. Conte D, Holcik M, Lefebvre CA, Lacasse E, Picketts DJ, Wright KE, Korneluk RG. Inhibitor of apoptosis protein cIAP2 is essential for lipopolysaccharide-induced macrophage survival. *Mol Cell Biol*. 2006;26:699–708.

16. Labbé K, McIntire CR, Doiron K, Leblanc PM, Saleh M. Cellular inhibitors of apoptosis proteins cIAP1 and cIAP2 are required for efficient caspase-1 activation by the inflammasome. *Immunity*. 2011;35:897–907.

17. Blanc-Brude OP, Teissier E, Castier Y, Lesèche G, Bijnens AP, Daemen M, Staels B, Mallat Z, Tedgui A. IAP survivin regulates atherosclerotic macrophage survival. *Arterioscler Thromb Vasc Biol*. 2007;27:901–907.

18. Moran EP, Agrawal DK. Increased expression of inhibitor of apoptosis proteins in atherosclerotic plaques of symptomatic patients with carotid stenosis. *Exp Mol Pathol*. 2007;83:11–16.

19. Boisvert WA, Spangenberg J, Curtiss LK. Treatment of severe hypercholesterolemia in apolipoprotein E-deficient mice by bone marrow transplantation. *J Clin Invest*. 1995;96:1118–1124.

20. Riches DW, Underwood GA. Expression of interferon-beta during the triggering phase of macrophage cytocidal activation. Evidence for an autocrine/paracrine role in the regulation of this state. *J Biol Chem*. 1991;266:24785–24792.

21. Mosmann T. Rapid colorimetric assay for cellular growth and survival: application to proliferation and cytotoxicity assays. *J Immunol Methods*. 1983;65:55–63.

22. Daugherty A, Whitman SC. Quantification of atherosclerosis in mice. *Methods Mol Biol*. 2003;209:293–309.

23. Horrevoets AJG, Fontijn RD, van Zonneveld AJ, de Vries CJM, ten Cate JW, Pannekoek H. Vascular endothelial genes that are responsive to tumor necrosis factor-alpha in vitro are expressed in atherosclerotic lesions, including inhibitor of apoptosis protein-1, stannin, and two novel genes. *Blood*. 1999;93:3418–3431.

24. Cui X, Imaizumi T, Yoshida H, Tanji K, Matsumiya T, Satoh K. Lipopolysaccharide induces the expression of cellular inhibitor of apoptosis protein-2 in human macrophages. *Biochim Biophys Acta*. 2000;1524:178–182.

25. Rakesh K, Agrawal DK. Cytokines and growth factors in apoptosis and proliferation of vascular smooth muscle cells. *Int Immunopharmacol*. 2005;10:1487–1506.

26. Jia G, Aggarwal A, Tyndall SH, Agrawal DK. Tumor necrosis factor-a regulates p27 kit expression and apoptosis in smooth muscle cells of human carotid plaques via forkhead transcription factor O1. *Exp Mol Pathol*. 2011;90:1–8.

27. Mahoney DJ, Cheung HH, Mrad RL, Plenchette S, Simard C, Enwere E, Arora V, Mak TW, Lacasse EC, Waring J, Korneluk RG. Both cIAP1 and cIAP2 regulate TNFalpha-mediated NF-kappaB activation. *Proc Natl Acad Sci USA*. 2008;105:11778–11783.

28. Chu ZL, McKinsey TA, Liu L, Gentry JJ, Malim MH, Ballard DW. Suppression of tumor necrosis factor-induced cell death by inhibitor of apoptosis c-IAP2 is under NF-kappaB control. *Proc Natl Acad Sci USA*. 1997;94:10057–10062.

29. Samuel T, Welsh K, Lober T, Togo SH, Zapata JM, Reed JC. Distinct BIR domains of cIAP1 mediate binding to and ubiquitination of tumor necrosis factor receptor-associated factor 2 and second mitochondrial activator of caspases. *J Biol Chem*. 2006;281:1080–1090.

30. Zheng C, Kabaleeswaran V, Wang Y, Cheng G, Wu H. Crystal structures of the TRAF2:cIAP2 and the TRAF1:TRAF2:cIAP2 complexes: affinity, specificity and regulation. *Mol Cell*. 2012;38:101–113.

31. McComb S, Cheung HH, Korneluk RG, Wang S, Krishnan L, Sad S. cIAP1 and cIAP2 limit macrophage necroptosis by inhibiting Rip1 and Rip3 activation. *Cell Death Differ*. 2012;19:1791–1801.

32. Van Vlijmen BJ, Gerritsen G, Franken AL, Boesten LS, Kockx MM, Gijbels MJ, Vierboom MP, van Eck M, van De Water B, van Berkel TJ, Havekes LM. Macrophage p53 deficiency leads to enhanced atherosclerosis in APOE*3-Leiden transgenic mice. *Circ Res*. 2001;88:780–786.

33. Liu JJ, Huang RW, Lin DJ, Peng J, Wu XY, Lin Q, Pan XL, Song YQ, Zhang MH, Hou M, Chen F. Expression of survivin and bax/bcl-2 in peroxisome proliferator activated receptor-gamma ligands induces apoptosis on human myeloid leukemia cells in vitro. *Ann Oncol*. 2005;16:455–459.

34. Whitman SC. A practical approach to using mice in atherosclerotic research. *Clin Biochem Rev*. 2004;25:81–93.

35. Schrijvers DM, De Meyer GR, Kockx MM, Herman AG, Martinet W. Phagocytosis of apoptotic cells by macrophages is impaired in atherosclerosis. *Arterioscler Thromb Vasc Biol*. 2005;25:1256–1261.

36. Daniel JM, Sedding DG. Circulation smooth muscle progenitor cells in arterial remodeling. *J Mol Cell Cardiol*. 2011;50:273–279.

37. Clarke MC, Littlewood TD, Figg N, Maguire JJ, Davenport AP, Goddard M, Bennett MR. Chronic apoptosis of vascular smooth muscle cells accelerates atherosclerosis and promotes calcification and medial degeneration. *Circ Res*. 2008;12:1529–1538.

38. Zoll J, Fontaine V, Gourdy P, Barateau V, Vilar J, Leroyer A, Lopes-Kam I, Mallat Z, Arnal JF, Henry P, Tobelem G, Tedgui A. Role of human smooth muscle cell progenitors in atherosclerotic plaque development and composition. *Cardiovasc Res*. 2008;77:471–480.

39. Vu TH, Werb Z. Matrix metalloproteinases: effectors of development and normal physiology. *Genes Dev*. 2000;14:2123–2133.

40. Shai SY, Sukhanov S, Higashi Y, Vaughn C, Kelly J, Delafontaine P. Smooth muscle cell-specific insulin-like growth factor-1 overexpression in Apoe$^{-/-}$ mice does not alter atherosclerotic plaque burden but increases features of plaque stability. *Arterioscler Thromb Vasc Biol*. 2012;30:1916–1924.

41. Vukovic I, Arsenijevic N, Lackovic V, Todorovic V. The origin and differentiation potential of smooth muscle cells in coronary atherosclerosis. *Exp Clin Cardiol*. 2006;2:123–128.

42. Du C, Fang M, Li Y, Li L, Wang X. Smac, a mitochondrial protein that promotes cytochrome c-dependent caspase activation by eliminating IAP inhibition. *Cell*. 2000;102:33–42.

43. Verhagen AM, Ekert PG, Pakusch M, Silke J, Connolly LM, Reid GE, Moritz RL, Simpson RJ, Vaux DL. Identification of DIABLO, a mammalian protein that promotes apoptosis by binding to and antagonizing IAP proteins. *Cell*. 2000;102:43–53.

44. Wu G, Chai J, Suber TL, Wu JW, Du C, Wang X, Shi Y. Structural basis of IAP recognition by Smac/DIABLO. *Nature*. 2000;408:1008–1012.

45. Lu J, McEachern D, Sun H, Bai L, Peng Y, Qiu S, Miller R, Liao J, Yi H, Liu M, Bellail A, Hao C, Sun SY, Ting AT, Wang S. Therapeutic potential and molecular mechanism of a novel, potent, nonpeptide, Smac mimetic SM-164 in combination with TRAIL for cancer treatment. *Mol Cancer Ther*. 2011;10:902–914.

46. Petersen SL, Peyton M, Minna JD, Wang X. Overcoming cancer cell resistance to Smac mimetic induced apoptosis by modulating cIAP2 expression. *Proc Natl Acad Sci USA*. 2012;107:11936–11941.

47. Cossu F, Mastrangelo E, Milani M, Sorrentino G, Lecis D, Delia D, Manzoni L, Seneci P, Scolastico C, Bolognesi M. Designing Smac-mimetics as antagonists of XIAP, cIAP1, and cIAP2. *Biochem Biophys Res Commun*. 2009;378:162–167.

48. Cai Q, Sun H, Peng Y, Lu J, Nikolovska-Coleska Z, McEachern D, Liu L, Qiu S, Yang CY, Miller R, Yi H, Zhang T, Sun D, Kang S, Guo M, Leopold L, Yang D, Wang S. A potent and orally active antagonist (SM-406/AT-406) of multiple inhibitors of apoptosis proteins (IAPs) in clinical development for cancer treatment. *J Med Chem*. 2011;19:2714–2726.